# Dalton Transactions

Accepted Manuscript






ROYAL SOCIETY OF CHEMISTRY

www.rsc.org/dalton

Dalton Transactions

RSCPublishing

ARTICLE

# (3+1)-Dimensional commensurately modulated structure and photoluminescence properties of diborate $KSbOB_2O_5$

Dan Zhao*, Rong-Hua Zhang, Fei-Fei Li, Juan Yang, Bing-Guo Liu, Yun-Chang Fan

Cite this: DOI: 10.1039/x0xx00000x

Received ooth January 2012,
Accepted ooth January 2012

DOI: 10.1039/x0xx00000x

www.rsc.org/

ABSTRACT: Single-crystal of diborate $KSbOB_2O_5$ has been prepared under high temperature molten-salt method and its structure has been determined by single crystal X-ray diffraction analysis. Diffraction pattern show strong main reflections and weak satellite reflections, clearly indicating a modulated structure. Using the four-dimensional superspace formalism for aperiodic structures, its reflections can be indexed as orthorhombic superspace group $Pmn2_1(0\beta0)s00$ with the modulation vector **q** = 5/12 **b***, and then structure solution and refinement reached a final commensurately modulated model that were refined extremely well and does not show any unusual features. On the other hand, powder sample of $KSbOB_2O_5$ was synthesized by high-temperature solid state reaction method, and the powder X-ray diffraction pattern fits very well with the simulated from single-crystal date. In addition, photoluminescence properties of diborate $KSbOB_2O_5$ actived by 4.5 mol% $Dy^{3+}$ have been studied, indicating an extraordinary phenomenon that the red emission at around 635 nm ($^4F_{9/2}\rightarrow{}^6H_{11/2}$) is much stronger than the yellow emission at around 581 nm ($^4F_{9/2}\rightarrow{}^6H_{13/2}$).

## 1. Introduction

Searching for new second-order nonlinear optical (NLO) materials is of current interest and great importance due to their applications for solid state lasers to produce coherent light through cascaded frequency conversion.[1] From the viewpoint of fundamental understanding, the practical potential of materials is mostly associated with their structural characteristics. The necessary structural prerequisite for second harmonic generation (SHG) is crystallographic noncentrosymmetry (NCS). It was reported that the $\pi$-conjugated system based on trigonal $BO_3$ groups is responsible for the second harmonic generation (SHG) properties of the borates, such as $LnM_3(BO_3)_4$ (Ln=rare-earth element; M=Al, Ga, Cr, Fe, Sc) [2] and $ABe_2BO_3F_2$ (A = Na, K, Rb, Cs, Tl) [3]. On the other hand, introducing transition-metal ions susceptible to second-order Jahn-Teller (SOJT) distortions ($d^0$ transition metal ions, such as $Ti^{4+}$, $Nb^{5+}$, $Mo^{4+}$, or $W^{6+}$) and cations with nonbonded electron pairs ($Se^{4+}$, $Te^{4+}$, or $Sb^{3+}$) [4] into NCS compounds might also be SHG effective.

For this reason, it is meaningful to understand the detailed structure of a material for further studying its physical properties. Commonly, crystal structure of materials can completely be characterized by three basis vectors of the translational symmetry and the coordinates of the atoms in one unit cell. However, some solids are found in recent years which give distinct X-ray diffraction patterns but whose structures have no translational symmetry in the three-dimensional (3D) space. These so-called aperiodic crystals could be arbitrarily divided into the following three classes: modulated crystals, composite crystals and quasicrystals.[5]

Modulated and composite crystals have atomic structures that can be described as variations on periodic structures, while quasi-crystals differ from crystals with translational symmetry in a more fundamental way. All of these aperiodic crystals can be considered as periodic structures in a higher than 3D space.

In case of modulated crystals, the lacking translational periodicity in one, two, or three dimensions of the physical space can be described by one, two, or three modulation waves in different directions. To restore the periodicity, it is necessary to transform the data to (3 + n)D (n = 1, 2 or 3) spaces. Then the symmetry of modulated crystals can be described by so-called superspace groups in which the additional periodicities are treated as a new coordinate in a higher (3+n)D space. There are 4783 spacegroup types in four-dimensional (4D) space, 222018 spacegroup types in five-dimensional (5D) space and 28927922 spacegroup types in six-dimensional (6D) space, while there are only 219 spacegroup types in 3D space.[6]

In case of 4D modulated structures, atoms are no longer discrete objects, but 1D "atomic surfaces" and the reciprocal space vectors are generally expressed as $\mathbf{H} = h\mathbf{a}^* + k\mathbf{b}^* + l\mathbf{c}^* + m\mathbf{q}$ ($\mathbf{a}^*$, $\mathbf{b}^*$, and $\mathbf{c}^*$ are the basis vectors of the 3D reciprocal lattice). The modulation vector $\mathbf{q}$ can be expressed as $\mathbf{q} = \alpha\mathbf{a}^* + \beta\mathbf{b}^* + \gamma\mathbf{c}^*$, where $\alpha$, $\beta$, and $\gamma$ are numbers which are rational for commensurate cases and irrational for incommensurate cases. In this view, four reciprocal vectors ($\mathbf{a}^*$, $\mathbf{b}^*$, $\mathbf{c}^*$, $\mathbf{q}$) in 3D space are considered to be the projection of four reciprocal basis vectors in 4D space. Many modulated structures have been solved properly in recent years, such as 2H-$NbSe_2$,[7] $[Bi_{0.84}CaO_2]_2[CoO_2]_{1.69}$,[8] $[CaNd]_2[Ga]_2[Ga_2O_7]_2$,[9] $Lu_4AlCu_2B_9O_{23}$,[10] $\beta$-$TcCl_2$,[11] $REe_7$(RE = La, Ce, Pr, Nd, Sm),[12] $Eu(Zn_{1-x}Ge_x)_2$,[13] $\delta''$-$Au_{1+x}Cd_{2-x}$,[14] $Sr_2Fe_2O_5$,[15] $LiFeBO_3$,[16] $([SnSe]_{1.16})_1(NbSe_2)_1$,[17] and $Zr_2Co_{11}$[18] etc.

A series of pyroborate with the general formula $AMOB_2O_5$ (A=K, Rb, Cs, Tl; M = Nb, Ta, Sb) have been reported for their crystallographic NCS and potential applications as Second-Order Nonlinear Optical (NLO) materials.[19] These compounds are based on a common underlying basic structure with the orthorhombic spacegroup $Pmn2_1$ and unit cell $a \approx 7.33$ Å, $b \approx 3.84$ Å, $c \approx 9.30$ Å, and feature a 3D framework resulting from the condensation of $MO_6$ octahedra, irregular $AO_8$ polyhedra and $B_2O_5$ groups. On the other hand, it has been found that some of these compounds exhibit superstructures of varying multiplicities along the *b*-axis, such as $CsTaOB_2O_5$ with eightfold superstructure,[20] $TlNbOB_2O_5$ with twofold superstructure,[21] $RbNbOB_2O_5$ with fivefold superstructure,[22] and $KNbOB_2O_5$ with eightfold superstructure [23]. Alternatively, these compounds feature (3+1)D commensurately modulated structure of varying modulation vectors. Although crystallographic methods for analysing 3D periodic structures can be used to study commensurately modulated crystals according to a superlattice of the basic structure, structure determination and structure refinement of superstructures may be difficult to impossible for the weaker intensity of satellite reflections than that of main reflections. The more scientific approach for analyzing commensurately modulated compounds is superspace formalism for aperiodic structures. For the first time, Schmid et al used this approach for this family of compounds to refine the structure of $RbNbOB_2O_5$ with superspace group symmetry $Pmn2_1(0,0.4,0)s00$, resulting in the overall R value substantially lower than for the superstructure refinement.[22] Schmid and Wagner also determined the superspace group symmetry of $KNbOB_2O_5$ to be $Pmn2_1(0,0.375,0)s00$ by analyzing the extinction condition.[23] However, the final refinement for $KNbOB_2O_5$ was fulfilled using superstructure approach.

Among this family, compound $KSbOB_2O_5$ has been reported by Huang et al. for a polar material that displays weak SHG response.[24] Its crystal structure was determined to be NCS space group *Cc* which showed a little difference comparing with the other compounds of $AMOB_2O_5$ family. Such a structure character promoted us to study the diffraction pattern to confirm whether structure modulation exists in $KSbOB_2O_5$. By using high temperature molten salt method, we synthesized the single crystals of $KSbOB_2O_5$ whose structure is commensurately modulated and in agreement with the basic structure type of most compounds of $AMOB_2O_5$ family. We think Huang's report is another phase of $KSbOB_2O_5$, which is basically isotype but a little different from our results. In this work, we will report single crystal growth by molten salt method, structural determination by single-crystal X-ray diffraction analysis, and photoluminescence properties (activated by $Dy^{3+}$) of $KSbOB_2O_5$.

## 2. Experimental Section

### 2.1 Materials and instrumentation

All of the chemicals were analytically pure from commercial sources and used without further purification. $K_2B_4O_7$, $K_2CO_3$, $H_3BO_3$, $Dy_2O_3$, and $Sb_2O_5$ were purchased from the Shanghai Reagent Factory. The morphology of the samples as well as microprobe elemental analyses was examined by Scanning Electron Microscopy (SEM) images taken with a Quanta 200FEG scanning electron microscope equipped with an energy-dispersive X-ray spectroscope (EDS). X-Ray powder diffraction (XRD) patterns were collected on a Rigaku DMax-2500/PC powder diffractometer by using graphite-monochromated CuK$\alpha$ radiation in the angular range $2\theta$ = 5~75° with a step size of 0.02°. UV-Vis diffuse reflectance spectra (DRS) were recorded on a UV-Vis spectrophotometer (JASCOV-550) equipped with an integrating $BaSO_4$ sphere in the wavelength range of 250~750nm at room temperature. The excited and emission spectrums were measured on a Cray Eclipse fluorescence spectrometer using Xe lamp at room temperature.

### 2.2 Syntheses

Single crystals of $KSbOB_2O_5$ were prepared by molten salt method by using $K_2B_4O_7$ as flux, which is a little difference from Huang's report. As initial reagents, the mixture of $K_2B_4O_7{\cdot}4H_2O$ (2.000 g, 6.547 mmol) and $Sb_2O_5$ (0.212 g, 0.655 mmol) was thoroughly ground in an agate mortar and pressed into a pellet to ensure the best homogeneity and reactivity. Secondly, the mixture was put into a platinum crucible and was transferred into an oven and heated at 900°C in the air for 20 h. The mixture was completely melted in this stage, which was then allowed to cool at a rate of $4^oC{\cdot}h^{-1}$ to 600°C before



 

switching off the furnace. After boiling in water, plate-shaped colourless crystals were purified in very low yield (<10 %).

After proper structural analysis, pure powder sample of title compound was obtained quantitatively by the traditional solid state reaction of a mixture of $K_2B_4O_7/Sb_2O_5$ in a molar ratio of 1 : 1. The mixture was thoroughly ground in an agate mortar and pressed into a pellet. Then it was calcined in a platinum crucible for 48 h at 700°C, with several intermediate grinding stages to ensure a complete solid state reaction. The purity of powder pattern was confirmed by power XRD diffraction studies.

4..5 mol% Dy-dpoed $KSbOB_2O_5$ was prepared by the similar method. A mixture of $K_2CO_3/Dy_2O_3/H_3BO_3/Sb_2O_5$ with a molar ratio of 0.0955/0.015/4/1 was used as the raw materials, which were thoroughly mixed and preheated at 300°C for 4 h to decompose $K_2CO_3$ and $H_3BO_3$. Then it was calcined in a platinum crucible for 48 h at 700°C, with several intermediate grinding stages to ensure a complete solid state reaction. The purity of powder pattern of Dy-dpoed $KSbOB_2O_5$ was also confirmed by power XRD diffraction studies.

### 2.3 Single-crystal X-ray diffraction analysis

A suitable single crystal with dimensions of 0.20×0.20×0.05 mm was selected and mounted on a glass fiber for the single-crystal X-ray diffraction experiments. A set of intensity data was collected using a Bruker Smart APEX II CCD [25] single-crystal diffractometer system equipped with a graphite-monochromated *Mo-Kα* radiation source (λ = 0.71073 Å) over an angular range of 1.776 — 28.273 ° with an exposure time of 40 s·deg$^{-1}$. The frames were collected at ambient temperature with a scan width of 0.5° in $\omega$ and integrated with the *Bruker SAINT* software package using a narrow-frame integration algorithm. Diffraction patterns show strong main reflections and weak satellite reflections, clearly indicating a modulated structure. Using the tool of RLATT, the reciprocal space constructed from the experimental single crystal diffraction data of compound $KSbOB_2O_5$ could be described in Fig. 1, showing the main reflections, satellite reflections and modulation vectors along the *a*-, *b*- and *c*-axis. Then the main reflections were indexed on the basis of a triclinic unit cell, and the satellite reflections besides the normal Bragg reflections were indexed considering a commensurate modulation. According to high-dimensional crystallography, reflections could be indexed with four integers as $\mathbf{H} = h\mathbf{a}^* + k\mathbf{b}^* + l\mathbf{c}^* + m\mathbf{q}$ with $a$ = 7.1133(5) Å, $b$= 3.6883(10) Å, $c$ = 9.4096(14) Å and $\mathbf{q}$ = 0.41667 $\mathbf{b}^*$ up to the order |m| = 1 (reflections with |m| = 2 are very weak and are not refined). As the component of the $\mathbf{q}$ vector is very similar to rational number 5/12, the structure could be considered to be commensurately modulated. After that, the unit cell parameters were refined on the process of integrating using the main reflections and the first order satellite reflections. The scale module, deployed within Apex II, was used for multi-scan absorption corrections and generating *.p4p and *.hk6 files for structure solution. After that, the crystal structure of title complex was solved directly in superspace by the charge-flipping method using the *Superflip* program [26] assuming kinematical diffraction intensities and subsequently refined by the *JANA2006* crystallographic computing system.[27] The details of the data collection and structure refinement are summarized in Tab. 1, and the further details of the crystal structure investigations can be obtained from the Fachinformationszentrum Karlsruhe, 76344 Eggenstein-Leopoldshafen, Germany (fax: (49)7247-808-666; e-mail: crysdata@fizkarlsruhe.de), on quoting the depository numbers of CSD-428848.

## 3. Results and discussion

### 3.1. Structure solution and refinement

Early studies on modulated crystals mainly relied on polycrystalline X-ray diffraction, synchrotron radiation diffraction, or neutron diffraction. However, it is usually difficult to fully interpret the crystal structure of a modulated crystal. Single-crystal X-ray diffraction analysis is no doubt a reliable technique to determine 3-D structures as well as (3+n)D (n=1, 2, or 3) modulated structures using high-dimensional crystallographic approach. For commensurate cases, the structure could usually be solved by superstructure method. However, structure determination and refinement using superstructure method may be very difficult if satellite reflections are too weak especially for superlattice with a high multiple. For $KSbOB_2O_5$ with the modulation vector of 5/12 $\mathbf{b}^*$, a 12 times supercell has to be used for superstructure model, so that scattering information is hardly sufficient to fix the higher-order satellites. As a trial, we used superstructure model to solve and refine the structure of $KSbOB_2O_5$ but failed. Hence, the more scientific and effective approach, superspace formalism was used to solve and refine the commensurately modulated structure of $KSbOB_2O_5$.

Higher dimensional space groups were tested using the *Jana2006* software, and it was found that all observed reflections fulfilled the reflection conditions for the 4D superspace group $Pmn2_1(0\beta0)s00$ , a space group that belongs to the (3 +1)D subset of 4D space groups. In this nomenclature, the $Pmn2_1$ component indicates that the (3 + 1)D symmetry operations are derived from this 3D space group, and the "$(0\beta0)$" tells us that the $\mathbf{q}$ vector have one componentson of $\mathbf{b}^*$. Within 4D superspace formalism approach, the additional coordinates $x_4$ can be expressed as $x_4 = t + \mathbf{q}\cdot\mathbf{x}$, where $\mathbf{x} = (x_1, x_2, x_3)$ are the physical-space coordinates with respect to the lattice, and $t$ ($0 \leq t \leq 1$) parameter are the distance between a point and physical space. The structure solution that was performed using the program *Superfip* assuming kinematical diffraction intensities, generated 7 atomic positions in the asymmetric unit. Extinction correction, anisotropic displacement parameters, and one positional modulation of all the atomic positions were applied at this stage. The output of the charge-flipping procedure is a scattering density map that can be interpreted in terms of atomic positions by *Jana2006* to locate in the density not only the atomic positions but also the

modulation functions. After that, improvements to the model were made from inspection of the electron density maps surrounding the atomic positions where the initial assignments of the *Jana2006* program did not suffice. Fourier syntheses indicated that, all atoms except $O^1$ and $O^4$ atoms were only moderately modulated, and they can be described by several harmonic waves of positional modulation in the model, as shown in Fig. 2.

As shown in Fig. 3, superspace density map obtained by charge flipping revealed that $O^1$ and $O^4$ atoms showed a discontinuity, respectively in the modulation function. Thus the parameters of the special modulation functions (sawtooth and crenel functions) should be considered. Through trial and error we deduced that the discontinuities could be modelled by shifting the $O^1$ and $O^4$ atoms from the special positions on the mirror planes and describing their modulations by crenel functions of width 0.5.[28] The action of the mirror planes, which include a shift of 0.5 along the internal dimension, generates the complementary part of the atomic domains, so that the total occupations of the $O^1$ and $O^4$ atoms are 1 for the whole interval of $x_4$.

The final agreement factors converged to the excellent values of around 3.6% for all observed reflections (including 648 main and 771 satellite reflections) ($I > 3\sigma(I)$) and around 4.9% ($\omega R$) for all reflections, with all atoms in the structure refined using harmonic anisotropic atomic displacement parameters (ADP). Difference Fourier syntheses using the final atomic parameters showed no significant residual peaks (highest residual peak of 0.33 e·Å$^{-3}$ and highest residual hole -0.53 e·Å$^{-3}$). Therefore, our commensurately modulated refined model for $KSbOB_2O_5$ is reasonable.

Moreover, the accuracy of our (3+1)D commensurately modulated structure model can be confirmed by powder diffraction analysis. By using traditional high-temperature solid state reaction method, powder pattern of $KSbOB_2O_5$ can be obtained using for powder X-ray diffraction analysis. As shown in Fig. 4a, the simulated pattern fits very well with the experimental pattern in the $2\theta$ range of 5—65º. Although satellite reflections are very weak in powder diffraction pattern using Cu K$\alpha$ as the X-ray source, some satellite peaks can still be seen in some regions, such as (1 1 4 -1) and (3 0 -2 1), as shown in Fig. 4b. Hence, we can conclude that our structure model is correct and our powder pattern is pure.

### 3.2 Structural description.

Undoubtedly, the average structure of $KSbOB_2O_5$ (noted as $KSbB_{ave}$) represents the parent structure of $AMOB_2O_5$ family. As shown in Fig. 5a, $KSbB_{ave}$ features a 3D anionic boroantimonate network of $[SbOB_2O_5]_\infty$ which delimits holes filled by $K^+$ cations to ensure the cohesion and the neutrality of the structure. There are one unique potassium (I) atoms, one unique stibium (V) atom, one unique boron (III) atom, and four oxygen (II) atoms in the asymmetric unit of the average structure. Each Sb atom is octahedrally coordinated by two $O^1$, two $O^2$ and two $O^3$ atoms into a $SbO_6$ octahedron. $SbO_6$ octahedra are interconnected via corner-sharing $O^1$ atoms to form an infinite 1D chain along the *b*-axis. It should be noted that in the average structure the bridging $O^1$ atoms split into two positions which are related by a slide plane. This phenomenon arouses from the strong crenel-like modulation of $O^1$ atom, and in modulated structure such splitting will be removed. $B^1$ atoms are three-coordinated by $O^2$, $O^3$, and $O^4$ atoms in a nearly planar triangular geometry with the torsion angle about 177.9º for $O^2$–$B^1$–$O^3$–$O^4$. Then two adjacent $BO_3$ units are connected via corner-sharing $O^4$ atoms to form nearly planar $B_2O_5$ units. Remarkably, $O^4$ atom displays crenel-like modulation similar to $O^1$ atoms, so the positional splitting in average structure will not present in 4D description.

Furthermore, 1D chains of are bridged by $B_2O_5$ groups forming an anionic 3D network of $[SbOB_2O_5]_\infty$ (Fig. 6A) with large holes filled by $K^+$ cations to maintain electrical neutrality. In view of topology, the $B_2O_5$ group connected by three $SbO_6$ octahedra can be considered as a three connected node, and $SbO_6$ octahedra connected by two other $SbO_6$ octahedra and three $B_2O_5$ groups can be considered as a five connected node. From this point of view, the 3D anionic network of $[SbOB_2O_5]_\infty$ can be described as a 3D 3,5-nodal net with Schläfli symbol of $\{6^3\}\{6^9.8\}$, as shown in Fig. 6B. Such a structural characteristic is essentially in agreement with other unmodulated phase of $AMOB_2O_5$ family, in which the K atoms, Sb atoms, and $BO_3$ groups make a straight line, respectively along the *b*-axis. With respect to Huang's report of $KSbOB_2O_5$ (Fig. 5B) with a monoclinic *Cc* symmetry (noted as $KSbB_C$), the basic 3D framework is similar, but the K atoms, Sb atoms, and $BO_3$ groups are not respectively in rectilinear form. And the two B atoms in $B_2O_5$ atoms are crystallographic distinct, thus breaking the minor plane to reduce the symmetry from orthorhombic to monoclinic. Another notable thing is, the $SbO_6$ octahedra in $KSbB_C$ have two directions array, while in $KSbB_{ave}$ the orientation of $SbO_6$ is unique, as shown in Fig. 5B.

The superspace formalism for modulated structures provides a way not only to solve and refine the structural features, but also to describe them in terms of a handful of meaningful structural parameters. In this approach, structure modulation breaks the 3D translation symmetry of $KSbB_{ave}$, resulting in the modulated structure $KSbB_{mod}$. Considering the modulation vector of 5/12, a 12 times supercell model can be used as an approximate representation of the atomic structure, as shown in Fig. 5C. In the 12 times commensurate cell description, the 1D chain of $SbO_6$ octahedra is no longer a straight line with unique $SbO_6$ orientation for the pushing of positional modulation, as shown in Fig. 7. And the coordinated configurations of $SbO_6$ octahedra become more regular than in the average structure. The distance between $Sb^1$ and $O^1$ atom whose strong modulation is described by crenel function in the 4D description is 1.95(3) Å on the average and is distributed between lengths of a minimum of 1.91(4) Å and maximum 2.03(4) Å. The detailed average $Sb^1$–$O^2$ and $Sb^1$–$O^3$ distances and their distributions are drawn in Fig. 8A and listed in Tab. 3. Similarly, the structural modulation breaks the perfect linear arrangement of the $B_2O_5$ groups into clusters in view along the *b*-axis, as shown in Fig. 5C. In the 12 times commensurate cell, the $B^1$–$O^2$ and $B^1$–$O^3$



 

bond distances are longer than the unit cell constant of 1.18 (12) and 1.32 (10) Å, respectively, achieving reasonable values as shown in Tab. 3 and Fig. 8B. $O^4$ atom that acts as the bridging atom in the $B_2O_5$ units shows the largest modulation with the $B^1$−$O^4$ bond distances distributed between 1.32(4) Å and 1.41(4) Å.

On the other hand, the $K^1$−O bonds especially the longest ones are strongly influenced by the positional modulation, whereby lengthening and shortening are imposed in different regions of the crystal, leading to the change in the coordinated environment of $K^1$ atom. As can be seen in Fig. 8C, 8D, 8E, 8F and Tab. 3, the longest bonds $K^1$−$O^{3i}$ display the largest modulations with the deviation of bond lengths up to 1.75 Å. The shorter K−O bonds display smaller K−O bond distributions imposed by modulations; the shortest K−O bond is $K^1$−$O^2$, showing the stretched average distance of 2.45(8) Å with deviation of only 0.38(2) Å.

It is useful to calculate the bond valence sums (BVS) to evaluate the validity of the commensurately modulated structure model. The average values in the modulated structure are 1.1423(4), 5.230(19) and 3.08(3) for $K^1$, $Sb^1$ and $B^1$ atoms, respectively, which are within a tolerable range and comparable with other potassium (I) compounds.[29]

### 3.3 Luminescence properties

The experimental optical diffuse reflectance absorption spectrum of $KSbOB_2O_5$ was measured ranging from 200 to 850 nm. As shown in Fig. 9, the absorption edges are around 370 nm and little absorption was observed in the range of 370−850 nm. Considering the wide band bap of $KSbOB_2O_5$, we think that it may be used as host material for light emitting applications. Hence, we prepared the Dy-doped $KSbOB_2O_5$ powder sample (noted as $K_{0.955}SbOB_2O_5$ : Dy 0.015) and studied its luminescence properties.

Fig. 10A shows the excitation spectrum of $K_{0.955}SbOB_2O_5$ : Dy 0.015 phosphor sintered at 700ºC for 24h. The excitation data of the main blue fluorescence ($\lambda_{em}$ = 463 nm) are recorded from 300 to 400 nm. There are two intense and sharp lines around 338 and 365nm, which correspond to f–f transitions within $Dy^{3+}$. The peak intensity at 365nm corresponding to transition from the $^6H_{15/2}$ ground state to $^6P_{5/2}$ is the strongest among the peaks.

The emission spectra of $K_{0.955}SbOB_2O_5$ : Dy 0.015 excited at 365nm is shown in Fig. 10B. There were two strong emissions centered at 463 nm (blue) and 635 nm (red) and a weak emission at around 581 nm (yellow), which could be ascribed to the $^4F_{9/2}\rightarrow{}^6H_{15/2}$, $^4F_{9/2}\rightarrow{}^6H_{13/2}$ and $^4F_{9/2}\rightarrow{}^6H_{11/2}$ transitions of $Dy^{3+}$, respectively. From the viewpoint of fundamental understanding, the outside environment of $Dy^{3+}$ strongly affects the intensity of transition.[30] Yellow emission at about 581 nm is well-known as a hypersensitive transition and is a force delectric dipole transition whose intensity depends on if the $Dy^{3+}$ cations occupy the inversion centre sites. Unlikely, blue emission at about 463 nm is magnetic dipole allowed, which has the maximum intensity if $Dy^{3+}$ cations occupy sites with inversion centre symmetry in the crystal field. Hence, different ratios of yellow-to-blue (Y/B) can be obtained by selecting host materials to obtain white-light emission. For $K_{0.955}SbOB_2O_5$ : Dy 0.015, $Dy^{3+}$ cations substitute sites of $K^+$ cations which is not the inversion centre sites. However, yellow emission is much weaker than blue and red emissions. The result may be ascribed to the function of the hole or electron traps produced by substitution of the univalent $K^+$ cations in the matrix aliovalently with trivalent $Dy^{3+}$ cations.[31] On the other hand, the red emission is only a little weaker than the blue emission in $K_{0.955}SbOB_2O_5$ : Dy 0.015, which is comparable than other reported $Dy^{3+}$ activated fluorescent materials.[32] In summary, we think that such a character makes it may act as a potential white-light emitting material which can supply adequate red emissions.

## 4. Conclusions

A new phase of $KSbOB_2O_5$ belonging to $AMOB_2O_5$ (A=K, Rb, Cs, Tl; M = Nb, Ta, Sb) family was synthesized not only for single crystals but also for powder pattern. The results of single-crystal X-ray diffraction analysis revealed that it is a (3+1)-dimensional commensurate modulated structure and is structural distinct with Huang's report of monoclinic phase which is active for SHG response.[24] For the first time, the structure of $AMOB_2O_5$ family compounds was interpreted by high-dimensional crystallographic approach. With superspace group $Pmn2_1(0\ 0.41667\ 0)s00$, the structure solution and refinement reach a final commensurately modulated model that are refined extremely well and does not show any unusual features. The powder X-ray diffraction pattern fits very well with the simulated from single-crystal date, proving that our structure model is correct and our powder pattern is pure. In addition, 4.5 mol% $Dy^{3+}$-doped $KSbOB_2O_5$ were synthesized by solid-state reaction and its photoluminescence properties were investigated. The blue and red emission gives the first and second strongest intensity, while yellow emission is much weaker than them.

## Acknowledgements

This work was supported by National Science Foundation of China (Grant No. 21201056; 21307028; 11204067).

## Notes

Address: Department of Physics and Chemistry, Henan Polytechnic University, Jiaozuo, Henan 454000, People's Republic of China
*Corresponding author: Dan Zhao (iamzd@hpu.edu.cn)

Electronic Supplementary Information (ESI) available: X-ray crystallographic file (CIF), See DOI: 10.1039/b000000x/

## REFERENCES

1. (a) C. T. Chen, Y. B. Wang, B. C. Wu, K. C. Wu ,W. L. Zeng and L. H. Yu, *Nature*, 1995, **373**, 322; (b) S. C. Wang, N. Ye, *J. Am. Chem. Soc*., 2011, **133**, 11458; (c) S. C. Wang, N. Ye, W. Li and D. Zhao, *J. Am. Chem. Soc.*, 2010, **132,** 8779; (d) C. Huang, C. L. Hu, X. Xu, B. P. Yang and J. G. Mao, *Inorg. Chem.*, 2013, **52**, 11551; (e) H. W. Yu, H. P. Wu, S. L. Pan, Z. H. Yang, X. L. Hou, X. Su, Q. Jing, K. R.

Poeppelmeier and J. M. Rondinelli, *J. Am. Chem. Soc.,* 2014**, 36**, 1264.
2. (a) W. X. You, Y. F. Lin, Y. J. Chen, Z. D. Luo and Y. D. Huang, *Opt. Mater.*, 2007, **29**, 488; (b) G. Jia, C. Tu, J. Li, Z. You, Z. Zhu and B. Wu, *Inorg. Chem.*, 2006, **45**, 9326; (c) S. C. Wang, N. Ye, *Solid State. Sci.*, 2007, **9**(8), 713.
3. (a) L. F. Mei, Y. B. Wang and C. T. Chen, *Mater. Res. Bull,* 1994, **29**, 81; (b) C. D. McMillen, J. W. Kolis, *J. Cryst. Growth*, 2008, **310**, 2033; (c) C. D. McMillen, J. Hu, D. VanDerveer and J. W. *Kolis, Acta. Crystallogr. Sect. B*, *2009*, **65**, 445.
4. (a) J. G. Mao, H. L. Jiang and F. Kong, *Inorg. Chem*, 2008, **47**, 8498; (b) A. Cammarata, W. G. Zhang, P. S. Halasyamani and J. M. Rondinelli, *Chem. Mater.*, 2014, **26**, 5773.
5. (a) T. Janssen, G. Chapuis and M. De Boissieu, *Aperiodic crystals: from modulated phases to quasicrystals. Oxford: Oxford University*, 2007; (b) S. Van Smaalen, *Incommensurate crystallography. Oxford Univ*, 2007.
6. (a) H. Brown, R. BuÈ low, J. NeubuÈ ser, H. Wondratschek and H. Zassenhaus, *Crystallographic Groups of Four-Dimensional Space; New York: Wiley*, 1978; (b) B. Souvignier, *Acta Crystallogr. Sect. A: Found. Crystallogr*, 2003, **59** (3), 210.
7. C. D. Malliakas, M. G. Kanatzidis, *J. Am. Chem. Soc.*, 2013, **135** (5) , 1719.
8. H. Muguerra, D. Grebille, E. Guilmeau and R. Cloots, *Inorg. Chem.,* 2008, **47** (7), 2464.
9. F. Wei, T. Baikie, T. An, M. Schreyer, C. Kloc and T. J. White, *J. Am. Chem. Soc.,* 2011, **133**, 15200.
10. P. A. Plachinda, E. L. Belokoneva, *Z. Anorg. Allg. Chem.*, 2008, **634**(11), 1965.
11. C. D. Malliakas, F. Poineau, E. V. Johnstone, P. F. Weck, E. Kim, B. L. P. M. Scott, Forster, M. G. Kanatzidis, K. R. Czerwinski and A. P. Sattelberger, *J. Am. Chem. Soc.*, 2013, **135** (42), 15955.
12. J. Zhang, P. H. Tobash, W. D. Pryz, D. J. Buttey, N. Hur, J. D. Thompson, J. L. Sarrao and S. Bobev, *Inorg. Chem.*, 2013, **52** (2), 953.
13. T. S. You, S. Lidin, O. Gourdon, Y. Wu and G. J. Miller, *Inorg. Chem.,* 2009, **48** (14), 6380.
14. P. P. Jana, S. Lidin, *Inorg. Chem.*, 2013, **52** (22), 12980.
15. J. E. Auckett, A.J. Studer, N. Sharma and C.D. Ling, *Solid State Ionics,* 2012, **225**, 432.
16. Y. Janssen, D. S. Middlemiss, S. H. Bo, C. P. Grey and P. G. Khalifah, *J. Am. Chem. Soc.,* 2012, **134** (30), 12516.
17. M.B. Alemayehu, M. Falmbigl, C. Grosse, K. Ta, S.F. Fischer and D. C. Johnson, *J. Alloys Compd.*,2015, **619**, 861.
18. X.Z. Li, W.Y. Zhang, D.J. Sellmyer, X. Zhao, M.C. Nguyen, C.Z. Wang and K.M. Ho, *J. Alloys Compd.,*2014, **611**, 167.
19. (a) M. Gasperin, Acta Crystallogr., Sect. B 30 (1974) 1181-1183; (b) A. Akella and D.A. Keszler, *J. Solid State. Chem.,*1995*,* **12**, 74; (c) P. Becker, L. Bohaty and R. Froehlich, *Acta Crystallogr., Sect. C: Cryst. Struct. Commun.,1995,* **51**, 1721; (d) G. M. Cai, W. Y. Wang, M. Li, Y.F. Lou, Y.P. Sun and X. L. Chen, *Mater. Res. Bull.*, 2009, **44**, 189.
20. P. Becker, L. Bohaty and R. Fröhlich, *Acta Crystallogr., Sect. C: Cryst. Struct. Commun.*, 1995, **51**, 1721.
21. M. Gasperin, *Acta Crystallogr., Sect. B: Struct. Sci.* 1947, **30,** 1181.
22. (a) A. Baucher, M. Gasperin and B. Cervelle, *Acta Crystallogr., Sect. B: Struct. Sci.,* 1976, **32**, 2211; (b) S. Schmid, R. L. Withers and D. Corker, *P. Baules. Acta Crystallogr., Sect. B: Struct. Sci.,2000,* **56**, 558.
23. S. Schmid, T. Wagner, *Acta Crystallogr., Sect. B: Struct. Sci.,* 2005, **61**, 361.
24. C. Huang, J. H. Zhang, C. L. Hu, X. Xu, F. Kong and J. G. Mao, *Inorg. Chem.,* 2014, **53**, 3847.
25. Bruker. APEX2 and SAINT, *Bruker AXS Inc., Madison, Wisconsin, USA,* 2008.
26. L. Palatinus, G. Chapuis, *J. Appl. Cryst.,* 2007, **40**, 786.
27. (a) Petricek, *V.; Dusek, M.; Palatinus, L. Jana,* 2006. (b) *Structure Determination Software Programs. Institute of Physics, Praha, Czech Republic.,* 2006; (c) *V. Petricek, M. Dusek, L. Palatinus, Z. Kristallogr.*, 2014, **229**(5), 345.
28. A. van der Lee, M. Evain, L. Monconduit, L. Brec, J. Rouxel and V. Petrícek, *Acta Crystallogr., Sect. B: Struct. Sci.,* 1994, **50**, 119.
29. (a) I. D. Brown, D. Altermatt, *Acta Crystallogr. Sect. B: Struct. Sci.,* 1985, **41**, 24; (b) N. E. Brese, M. O'Keeffe, *Acta Crystallogr. Sect. B: Struct. Sci.,* 1991, 47, 192; (c) S. J. Mills, A. G. Christy, E. C.-C Chen and M. Raudsepp, *Z. Kristallogr.,* 2009, **224**(9), 423.
30. (a) Q. Su, H. B. Liang, C. Y. Li, H. He, Y. H. Lu, J. Li, Y. Tao, *J. Lumin.,* 2007, **122-123**, 927-930; (b) K. V. Raju, C. N. Raju, S. Sailaja, S. J. Dhoble, B. S. Reddy, *J. Lumin.,* 2013, **134**, 297; (c) X. Li, L. Guan , M. S. Sun , H. Y. Liu , Z. p. Yang , Q. L. Guo and G. S. Fu, *J. Lumin.,* 2011, **131**, 1022; (d) D. Rajesh, M. DhamodharaNaidu and Y.C.Ratnakaram, *J. Phys. Chem. Solids*, 2014, **75**, 1210; (e) F. Zhang, T. Zhang, G. Q. Li and W. F. Zhang, *J. Alloys Compd.*, 2015, **618**, 484.
31. A.A. S. Alvania, F. Moztarzadehb, A. A. Sarabi, J. Lumin. 2005, 114, 131.
32. (a) F. L. Song, D. H. Chen, Y. H. Yuan, *J. Alloys Compd.*, 2008, **458**, 564; (b) P. Jena, S. K. Gupta, V. Natarajan, O. Padmaraj, N. Satyanarayana, M. Venkateswarlu. *Mater. Res. Bull.*, 2015, **64**, 223.



 

Table 1. Experimental Details for the Data Collection and Structural Refinement Details of $KSbOB_2O_5$

| | |
|---|---|
| Crystal data | |
| Chemical formula | $KSbOB_2O_5$ |
| $M_r$ | 278.5 |
| Crystal system, space group | Orthorhombic, $Pmn2_1(0\beta0)s00$ |
| Temperature (K) | 293 |
| Modulation wave vector | **q** = 5/12 **b*** |
| $a$, $b$, $c$ (Å) | 7.1133 (5), 3.6883 (10), 9.4096 (14) |
| $V$ (Å$^3$) | 246.87 (8) |
| $Z$ | 2 |
| abs coeff $\mu$ (mm$^{-1}$) | 6.38 |
| Crystal size (mm) | 0.20 × 0.20 × 0.05 |
| Data collection | |
| Diffractometer | Bruker CCD diffractometer |
| Absorption correction | Multi-scan |
| Radiation type | Mo $K\alpha$ |
| Wavelength (Å) | 0.71073 |
| range of $h$, $k$, $l$ and $m$ | $-9 \rightarrow h \rightarrow +9$ |
| | $-5 \rightarrow k \rightarrow +5$ |
| | $-12 \rightarrow l \rightarrow +12$ |
| | $-1 \rightarrow m \rightarrow +1$ |
| No. of measured, independent and observed [$I > 3\sigma(I)$] reflections | 6528, 1794, 1419 |
| No. of observed main reflections and first order reflections | 648, 711 |
| $R_{int}$ | 0.042 |
| $(\sin\theta/\lambda)_{max}$ (Å$^{-1}$) | 0.666 |
| Refinement | |
| $R$, $R\omega$ (obs) | 0.0358, 0.0489 |
| $R$, $R\omega$ (obs main reflections) | 0.0253, 0.0335 |
| $R$, $R\omega$ (obs first order satellite reflections) | 0.0599, 0.0682 |
| $GOF$ (obs) | 1.18 |
| No. of reflections and parameters | 1794, 121 |
| $\Delta\rho_{max}$, $\Delta\rho_{min}$ ($e$·Å$^{-3}$) | 0.33, −0.53 |
| Absolute structure | 843 of Friedel pairs used in the refinement |
| Symmetry operations: (1) $x_1, x_2, x_3, x_4$; (2) $-x_1, -x_2, -x_3, -x_4$ | |

Table 2. Fractional atomic coordinates and isotropic or equivalent isotropic displacement parameters (Å$^2$) for the average structure of $KSbOB_2O_5$

| | $x$ | $y$ | $z$ | $U_{iso}$*/$U_{eq}$ | Occ. (<1) |
|---|---|---|---|---|---|
| Sb1 | 0.5 | 0.94766 (16) | 0.00118 (18) | 0.0148 (2) | |
| K1 | 1 | 0.4856 (9) | −0.0910 (5) | 0.0337 (11) | |
| O1 | 0.428 (2) | 1.444 (3) | 0.029 (2) | 0.038 (7) | 0.5 |
| O2 | 0.710 (5) | 1.000 (8) | −0.136 (5) | 0.156 (16) | |
| O3 | 0.667 (6) | 0.896 (7) | 0.151 (4) | 0.217 (17) | |
| O4 | 0.927 (3) | 0.955 (6) | 0.168 (2) | 0.035 (5) | 0.5 |
| B1 | 0.804 (11) | 0.985 (12) | 0.239 (11) | 0.23 (5) | |

Table 3. Select interatomic distances in the modulated structure of $KSbOB_2O_5$

| Bonds | Average | Minimum | Maximum |
|---|---|---|---|
| Sb1—O1$^{i}$ | 1.96(3) | 1.91(4) | 2.03(4) |
| Sb1—O1 | 1.94(3) | 1.91(4) | 1.98(4) |
| Sb1—O1$^{ii}$ | 1.96(3) | 1.91(4) | 2.03(4) |
| Sb1—O1$^{iii}$ | 1.94(3) | 1.91(4) | 1.98(4) |
| Sb1—O2 | 1.99(2) | 1.94(2) | 2.06(2) |
| Sb1—O2$^{iii}$ | 1.99(2) | 1.94(2) | 2.06(2) |
| Sb1—O3 | 1.96(3) | 1.82(3) | 2.06(3) |
| Sb1—O3$^{iii}$ | 1.96(3) | 1.82(3) | 2.06(3) |
| K1—O1$^{iv}$ | 3.11(3) | 2.76(3) | 3.60(3) |
| K1—O1$^{ii}$ | 3.11(3) | 2.76(3) | 3.60(3) |
| K1—O2$^{i}$ | 2.99(2) | 2.76(2) | 3.19(2) |
| K1—O2 | 2.87(2) | 2.72(2) | 3.10(2) |
| K1—O2$^{v}$ | 2.99(2) | 2.76(2) | 3.19(2) |
| K1—O2$^{vi}$ | 2.87(2) | 2.72(2) | 3.10(2) |
| K1—O3$^{i}$ | 3.70(3) | 2.71(3) | 4.46(3) |
| K1—O3 | 3.48(3) | 2.77(3) | 4.33(3) |
| K1—O3$^{vii}$ | 3.38(3) | 2.73(3) | 4.17(3) |
| K1—O3$^{viii}$ | 3.70(3) | 2.84(3) | 4.36(3) |
| K1—O3$^{ix}$ | 3.38(3) | 2.73(3) | 4.17(3) |
| K1—O3$^{x}$ | 3.70(3) | 2.84(3) | 4.36(3) |
| K1—O3$^{v}$ | 3.70(3) | 2.71(3) | 4.46(3) |
| K1—O3$^{vi}$ | 3.48(3) | 2.77(3) | 4.33(3) |
| K1—O4$^{i}$ | 3.09(3) | 2.96(4) | 3.16(4) |
| K1—O4 | 2.91(3) | 2.89(4) | 2.94(4) |
| K1—O4$^{v}$ | 3.09(3) | 2.96(4) | 3.16(4) |
| K1—O4$^{vi}$ | 2.91(3) | 2.89(4) | 2.94(4) |
| B1—O2$^{xi}$ | 1.37(3) | 1.27(4) | 1.43(4) |
| B1—O3 | 1.36(4) | 1.25(4) | 1.44(4) |
| B1—O4 | 1.36(4) | 1.32(4) | 1.40(4) |
| B1—O4$^{vi}$ | 1.37(3) | 1.36(4) | 1.41(4) |

Symmetry codes: (i) $x_1, x_2-1, x_3, x_4$; (ii) $-x_1+1, x_2-1, x_3, x_4+1/2$; (iii) $-x_1+1, x_2, x_3, x_4+1/2$; (iv) $x_1+1, x_2-1, x_3, x_4$; (v) $-x_1+2, x_2-1, x_3, x_4+1/2$; (vi) $-x_1+2, x_2, x_3, x_4+1/2$; (vii) $-x_1+3/2, -x_2+1, x_3-1/2, -x_4+1/2$; (viii) $-x_1+3/2, -x_2+2, x_3-1/2, -x_4+1/2$; (ix) $x_1+1/2, -x_2+1, x_3-1/2, -x_4$; (x) $x_1+1/2, -x_2+2, x_3-1/2, -x_4$; (xi) $-x_1+3/2, -x_2+2, x_3+1/2, -x_4+1/2$.

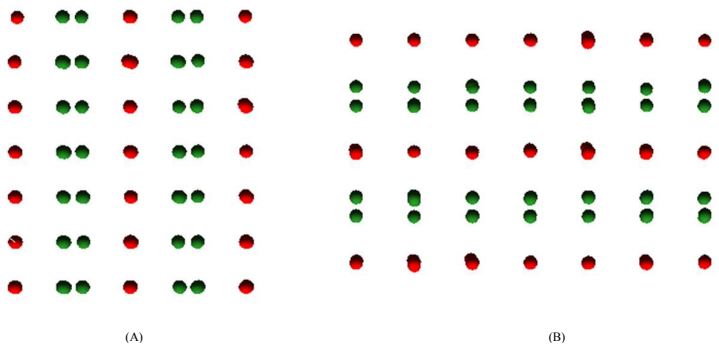

Figure 1. Reciprocal lattice view for $KSbOB_2O_5$ constructed from the experimental single crystal diffraction data showing the main reflections (red) and satellite reflections (yellow) down the *a*-axis (A) and *c*-axis (B).

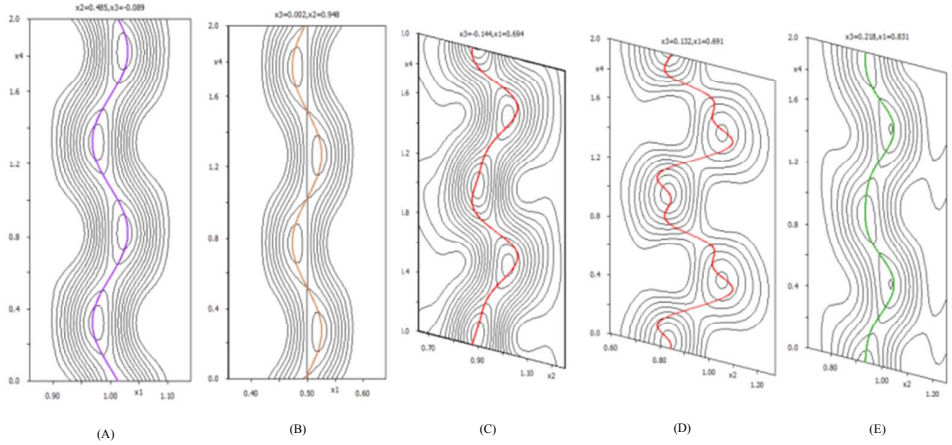

Figure 2. Positional modulations of $K^1$ (A), $Sb^1$ (B), $O^2$ (C), $O^3$ (D), $B^1$ (E) atoms in $KSbB_2O_5$ as functions of the internal $x_4$ axis through the superspace electron density.

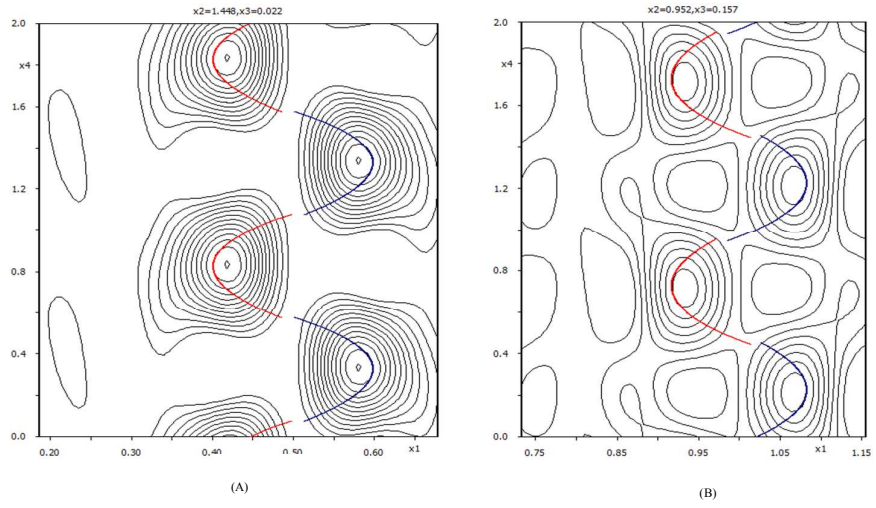

Figure 3. $x_1$–$x_4$ section through the superspace electron density at the position of the $O^1$ (A) and $O^4$ (B) atoms.

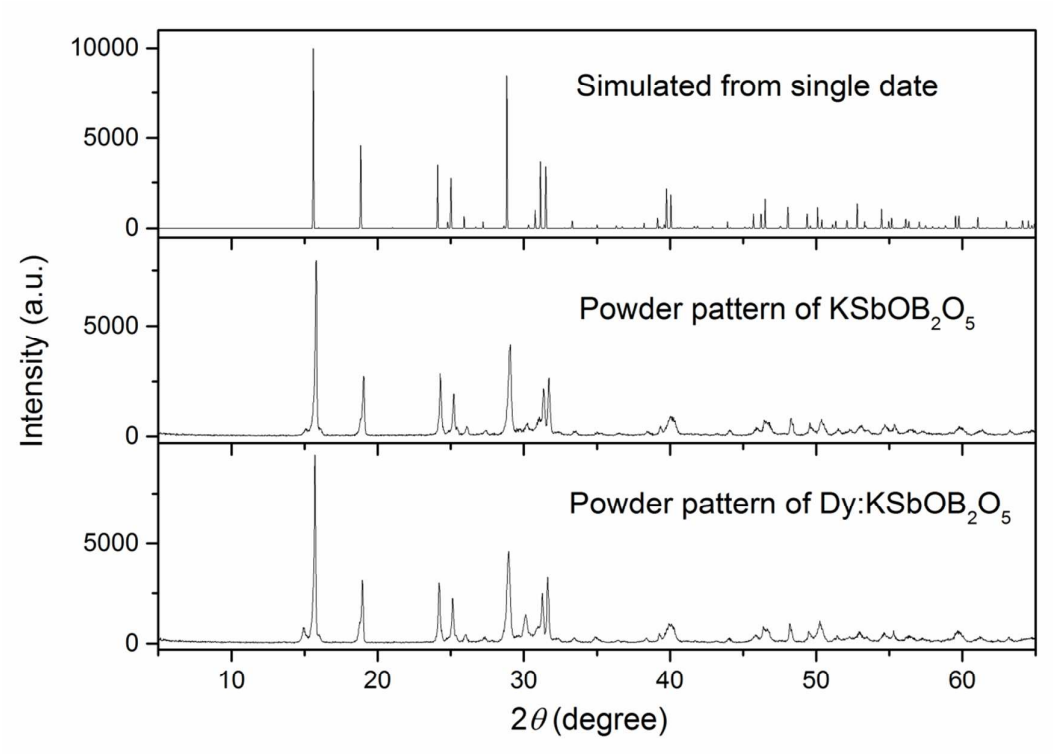


(A)

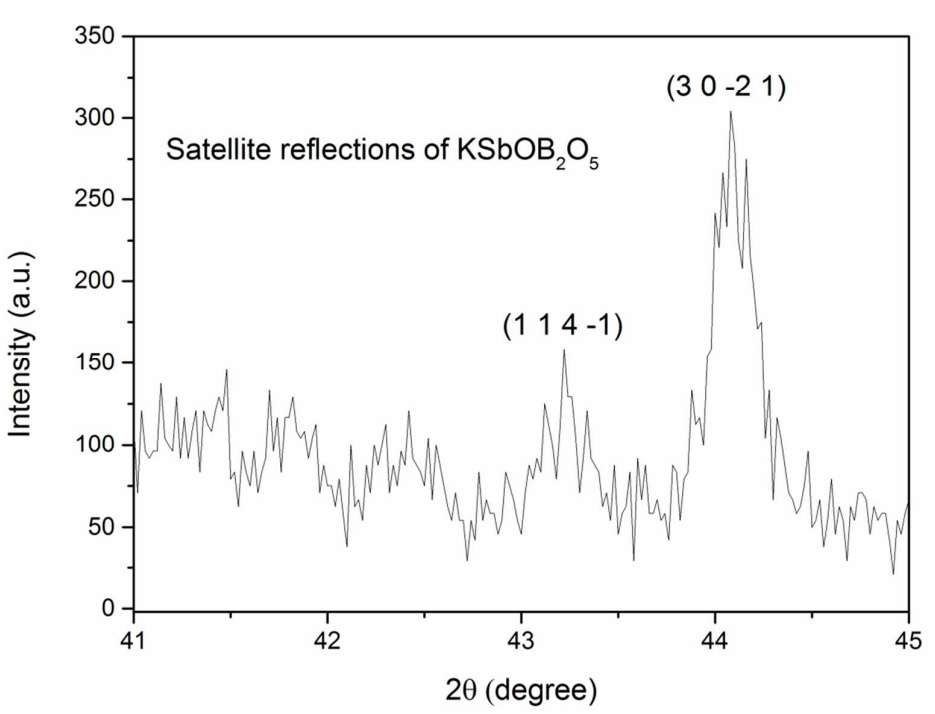


(B)

Figure 4. (A) Experimental and simulated X-ray powder diffraction patterns of $KSbOB_2O_5$ and Dy-doped $KSbOB_2O_5$ in the $2\vartheta$ range of 5—65º; (B) Experimental date of $KSbOB_2O_5$ in the $2\vartheta$ range of 41—45º to show the satellite peaks.

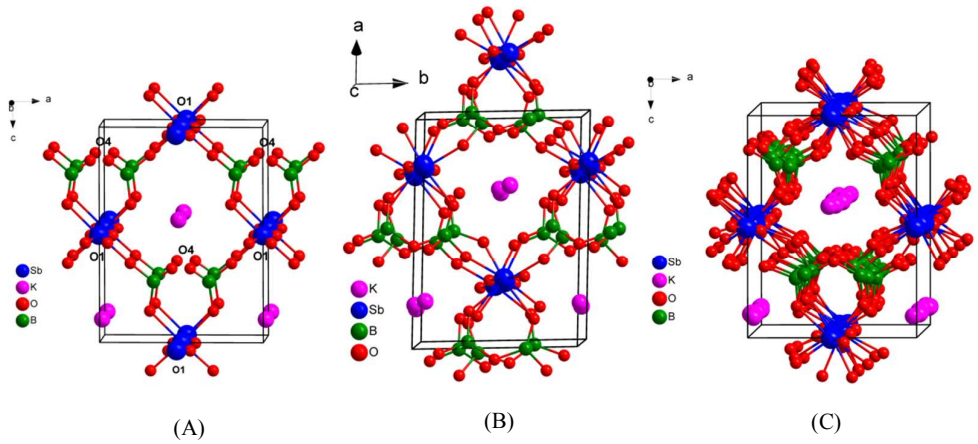


Figure 5. Average Structure (A), monoclinic phase (B) and 12 times supercell of commensurately modulated (C) of the $KSbOB_2O_5$ to show $SbO_6$ chains.

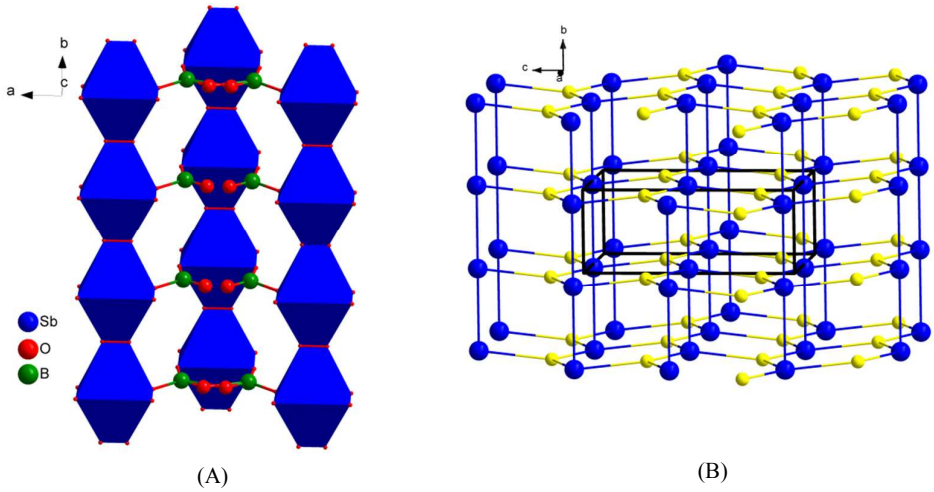


Figure 6. (A) The 3D anionic network of $[SbOB_2O_5]_\infty$ in the average structure of $KSbOB_2O_5$; (B) Topological view of the 3D 3,5-nodal net with Schläfli symbol of $\{6^3\}\{6^9.8\}$ for 3D anionic network of $[SbOB_2O_5]_\infty$

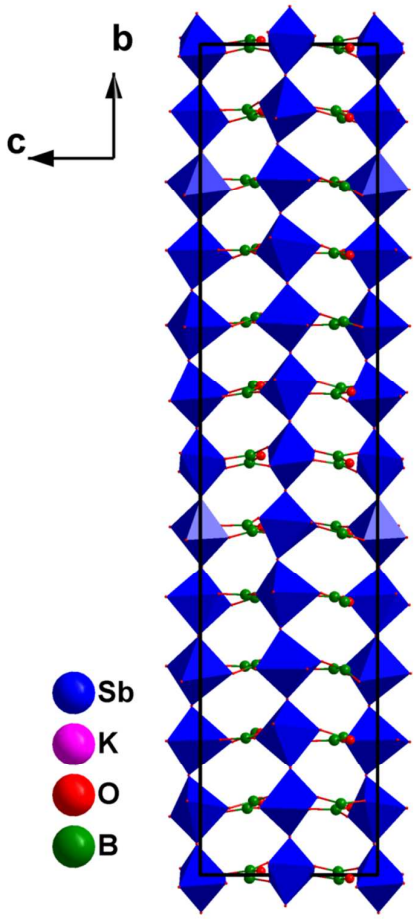


Figure 7. Supercell of the commensurately modulated of the $KSbOB_2O_5$ showing the positional modulations of $SbO_6$ octahedra.

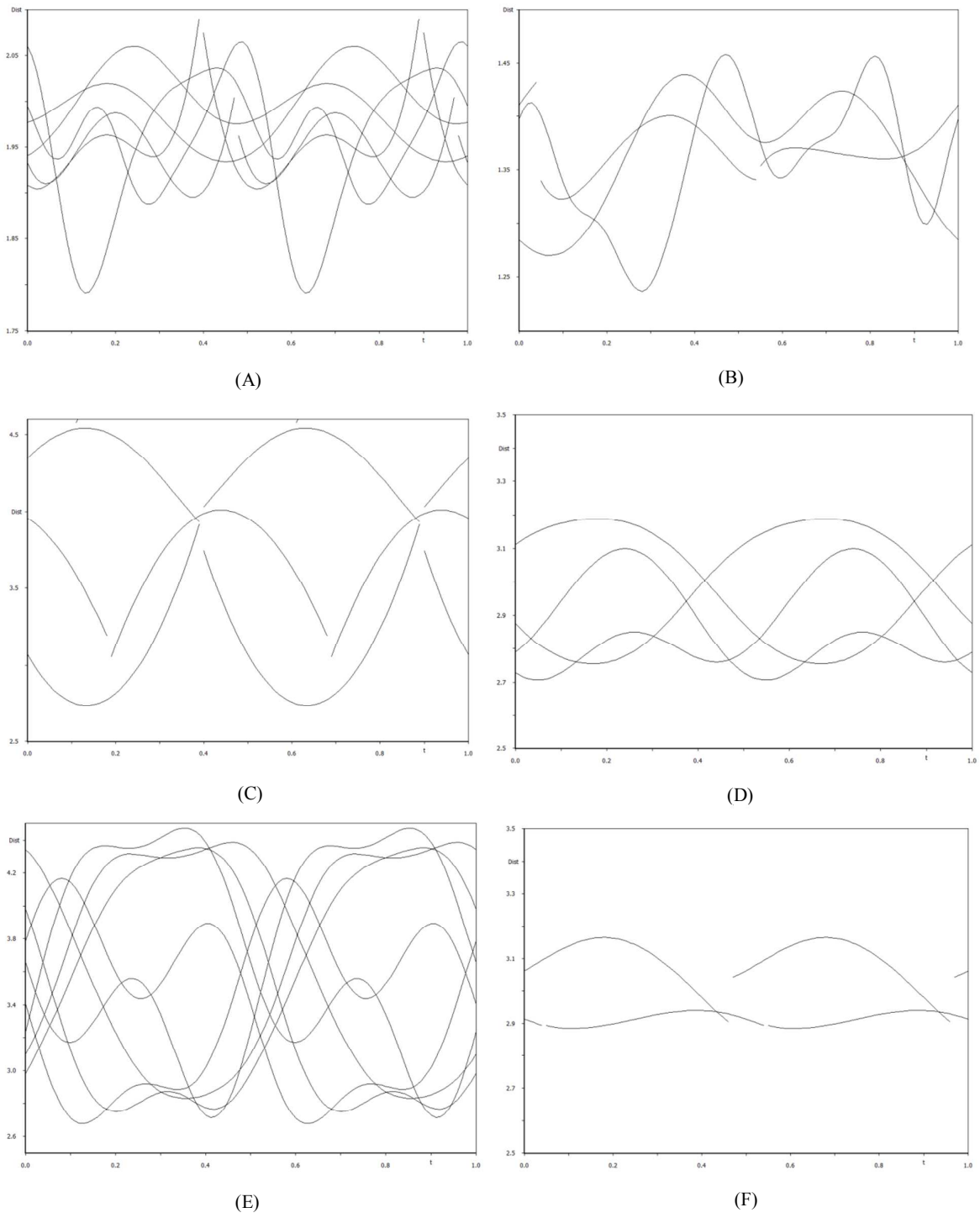


Figure 8. Evolution of $Sb^{1}$–O (A), $B^{1}$–O (B), $K^{1}$–$O^{1}$ (C), $K^{1}$–$O^{2}$ (D), $K^{1}$–$O^{3}$ (E) and $K^{1}$–$O^{4}$ (F) distances versus the internal parameter t

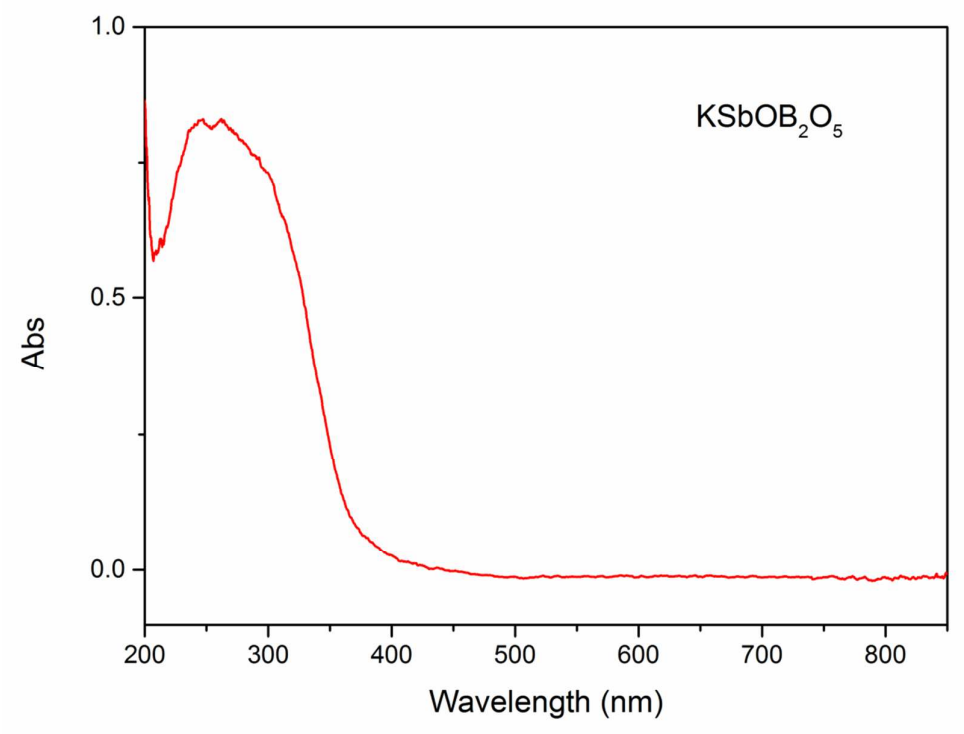


Figure 9. UV-Vis absorption spectra of $KSbOB_2O_5$ ranging from 200 to 850 nm.

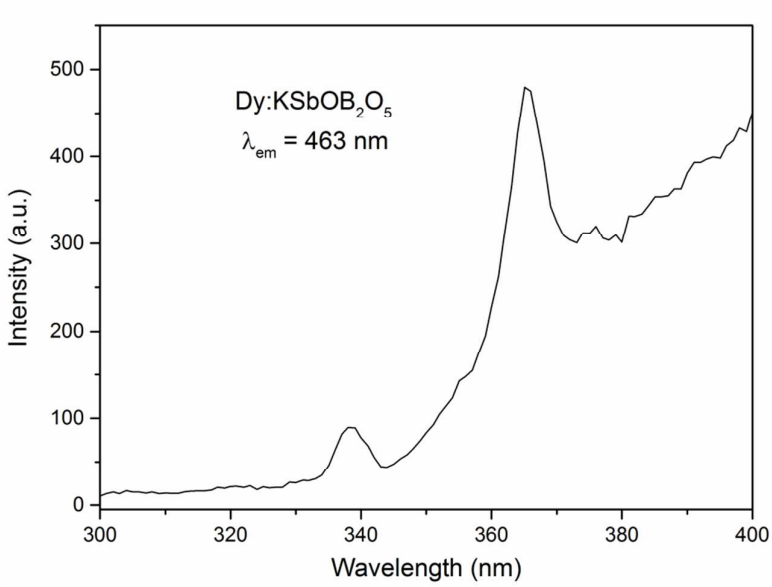


(A)

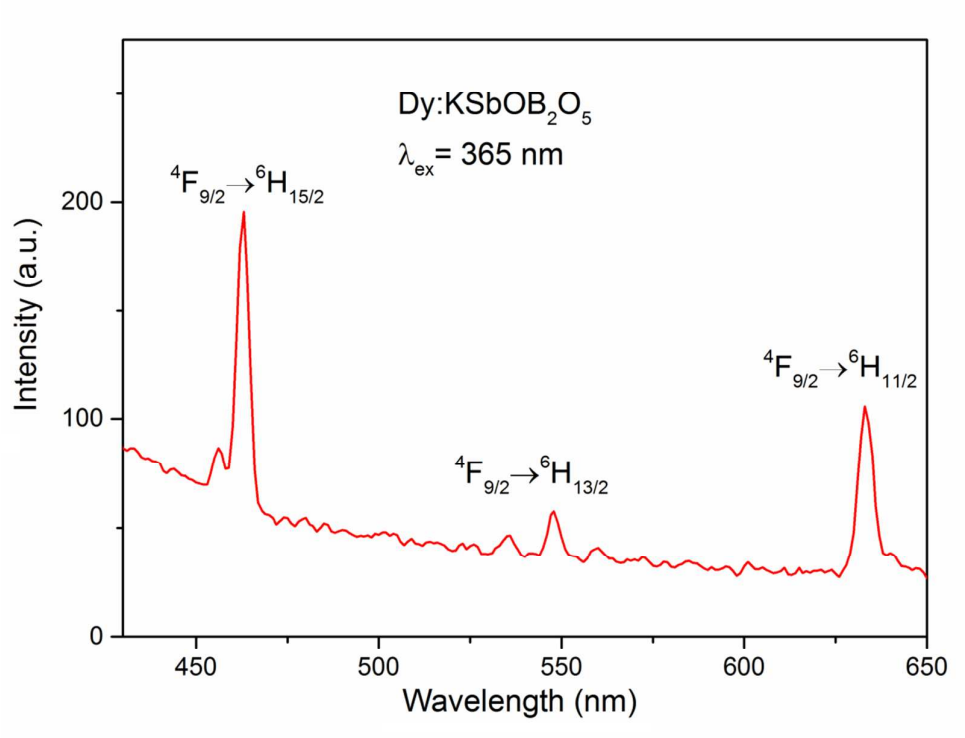


(B)

Figure 10. (A) Excitation spectra of $K_{0.945}SbOB_2O_5$ : Dy 0.015 ($\lambda_{em}$ = 463 nm); (B) Emission spectra of $K_{0.945}SbOB_2O_5$ : Dy 0.015 ($\lambda_{ex}$ = 365 nm)

This work reported the commensurately modulated structure of $KSbOB_2O_5$ using superspace formalism for aperiodic structures considering a modulation vector **q** = 5/12 **b***.